

Study of electrochemical hydrogen permeation in iron

^{1,*} E.Fallahmohammadi, ²A.Dolati, ³L.Lazzari, ⁴ F.Bolzoni

^{1,3,4}Politecnico di Milano, Dipartimento di Chimica, Materiali e Ingegneria Chimica “Giulio Natta”, via Mancinelli, 7, 20131 Milano, Italy.

²Sharif University of Technology, Department of material science and engineering, Azadi avenue, P.O Box, 11365 - 9466, Tehran, Iran.

Abstract

Hydrogen diffusion experiments in A106GR B carbon steel pipeline were performed electrochemically at 25°C in NACE,B, solution in various amount of sulfide ion concentration for a thin sample. In this case the effect of concentration of sulfide ion evaluated by study the electrochemical behavior of sample by the galvanostatic way. Generally, sulfur components were found to increase the hydrogen permeation rate. Presence of sulfide layer helped to absorption of hydrogen reduction and exacerbates the amount of hydrogen absorption in steel. this phenomena can be noted that as regard to analysis of corrosion products which formed in the surface sample, the high amount of FeS, The sulfide ion are believed to poison the steel surface which increases the chemical potential of adsorbed hydrogen on the surface. also hydrogen permeation test with the Devanathan and Stachurski, ASTM G148, permeation cell was prepared to evaluate the hydrogen diffusivity and permeation current behavior of steel pipe sample. The hydrogen diffusivity and subsurface concentration (C_{app}) were evaluated by fitting a series expansion of the diffusion equation to the permeation data. The hydrogen diffusivity in the steel was found to be approximately $9 \times 10^{-7} \text{ cm}^2/\text{s}$. The influence of the passive layer on the hydrogen permeation and its influence on the influence evaluation of diffusion and trapping characteristics were discussed.

Keywords: pipeline; Electrochemical hydrogen permeation; Hydrogen diffusivity; Hydrogen concentration

1.Introduction

Hydrogen dissolved in metals and alloys can cause detrimental effects on metallurgical and mechanical properties [1–6]. The effects are often referred to as hydrogen embrittlement and hydrogen blistering. Hydrogen embrittlement is a collective name for a number of different mechanisms, and therefore making it sometimes a rather confusing subject. High-strength alloys are often susceptible to one form of hydrogen embrittlement called hydrogen induced cracking (HIC) or hydrogen-induced stress cracking (HISC). The cracking mechanism involved in HIC is however a matter of much debate, since none of the proposed mechanisms has been generally accepted [7]. Lower-strength stainless steels of high ductility may also experience a reduction in tensile ductility but are generally free from HIC. In low-

alloy and carbon steel weldments one can find a form of HIC called underbead cracking. Rapid cooling of various carbon and low-alloy steels in the partially melted unmixed zone of the weldment produces martensite structures that are susceptible to HIC. Prevention requires careful selection of base-and weld-metal hardenability, cooling rate, and postweld treatment to keep hardness below specific levels. This became very evident at the Åsgard oil field during some failures in subsea oil and gas pipelines in the North Sea. The failures occurred as cracks at welds between low-alloyed carbon steel and 13Cr stainless steel tubes. In this case it was suspected that the failures could be explained by a combination of precipitation of brittle martensite in the heat affected zone of the weld, and hydrogen originating from cathodic protection of the carbon steel [8,9]. These problems have also led to new concepts when applying cathodic protection to offshore pipelines [10]. Generally, higher strength for pipeline steels involves lower SSC resistance. So far, there have been numerous efforts aimed at developing improved grades of pipeline steels with good SSC resistance in sour gas environments [11,12]. Most work concerning the effect of microstructure on H₂S resistance has dealt with the microstructures such as ferritic/perlitic microstructure, upper/lower bainite, quenched martensite and tempered martensite [13,14]. The increasing tendencies toward more severe environmental conditions and higher operating pressure have led to strict requirements for sour resistant pipeline steels. The susceptibility to hydrogen cracking is particularly related to the steel composition and the processing history as these parameters affect nonmetallic inclusions (type, size and morphology) and the material ability to accommodate hydrogen. Large inclusions such as elongated manganese sulfides and stringers of oxide increase the HIC susceptibility [15]. However, to be able to reduce the risk for hydrogen damage it is necessary to gain knowledge of the processes involved in the hydrogen uptake, and not only concentrate on the effects of hydrogen in materials. It is therefore important to investigate which factors that increase the hydrogen uptake in order to develop new methods and standards to prevent hydrogen damage in the future. The influence of H₂S on the cracking resistance as well as hydrogen permeation is previously investigated [16-19], and it is known that H₂S increases hydrogen absorption in steels probably due to a poisoning effect from HS⁻ on the surface [20,21]. However, many different theories describing the mechanism involved in the increased hydrogen absorption due to the surface poisons have been proposed [22,23]. The increase in hydrogen absorption obviously increases the subsurface hydrogen concentration, C_{app} , and hence also the permeation rate. Knowledge about how different conditions influence C_{app} is vital for the ability to estimate the risk for hydrogen related damages in different systems. Albeit being some of the most studied electrochemical processes, H electro adsorption and electro absorption are far from being well-understood at the atomic level [24]. The purpose of the present study was to investigate the effect of S²⁻ (sulphide) on hydrogen uptake and permeation in A106. Hydrogen concentrations and diffusivities in the steel membranes have been estimated by curve fitting a simple theoretical model to the experimental permeation data. The effect of various concentration of sulfide compounds are compared by evaluating the respective values for C_{app} .

2. Experimental

2.1. Material and experimental procedure

In this study, an electrochemical permeation technique was used to study the hydrogen transport in samples at the same thickness in 25 °C.

Samples were cut from 250 mm diameter A106 pipeline steel. The chemical composition of the steel is presented in Table 1. The samples were polished with SiC paper down to 1000

mesh, degreased in ethanol and dried in air. The thickness of the samples after polishing was 1.4 mm.

Table 1

chemical composition of A106 GRB carbon steel

C	Si	Mn	P	S	Cr	Mo
0.204	0.352	0.455	0.006	0.004	0.017	0.011

In the course of electrochemical permeation, hydrogen atoms were first absorbed at entry surface, then diffused through the metallic membrane, and were finally desorbed from the exit surface. on the entry surface, the production of hydrogen could be controlled galvanostatically or potentiostatically. on the exit surface, it is common to apply a constant potential to ensure that all hydrogen atoms could be ionized ,ensuring that the measured current density was the hydrogen flux.

The instrumentation of electrochemical hydrogen permeation was composed of an electrolytic cell with two compartments (cathodic side and anodic side), a reference electrode (saturated calomel electrode), an auxiliary electrode (wire of Pt),potentiostat/galvanostat (Fig. 1).

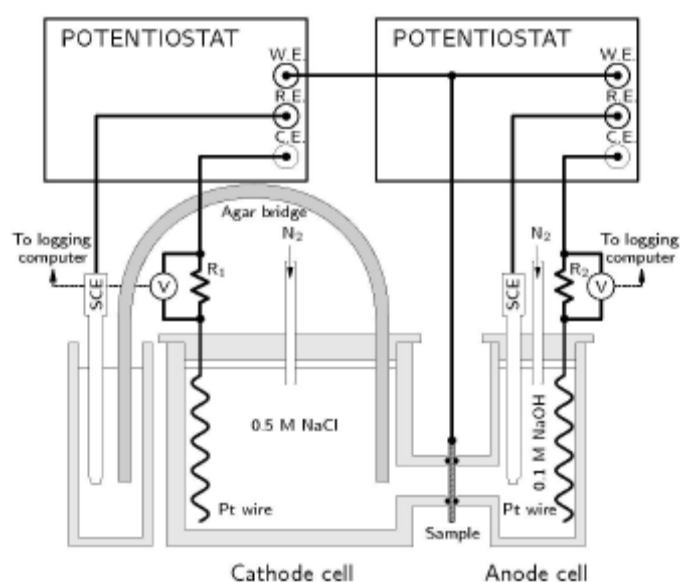


Fig1. Apparatus of electrochemical test.

The specimen (working electrode) was clamped between the compartments. One side of the specimen acted as the cathodic side, or hydrogen entry side, of the cell. It was galvanostatically polarized at a constant charging current density (2 mA/cm^2) in NaOH 0.1 M. The anodic side, or hydrogen exit side, of the cell was potentiostatically maintained at a constant potential of 0 versus reference electrode. This potential was sufficient to oxidize the hydrogen atoms emerging on the output face according to: $\text{H}_{\text{ads}} \rightarrow \text{H}^+ + \text{e}^-$.

The reference electrodes were standard Saturated Calomel Electrodes (SCE) and platinum wires with an exposed area of 4.5 cm^2 were used as counter electrodes. Rubber rings with a diameter of 16 mm sealed the connection between the sample and the cells leaving approximately 1.0 cm^2 of the sample exposed to the electrolytes in each cell. An agar bridge connected one of the reference electrodes to the cathode cell. The agar bridge was used to eliminate the risk of sulfur contamination of the reference electrodes during experiments.

The anodic current (exit side) gave a direct measure of the hydrogen flow rate J (permeation flux), is proportional to the anodic current (I_p) detected in this face. Solutions on both cells of the membrane were continuously deoxygenated by (Argon) bubbling before the addition of sulfide compound. the measurement was stopped 20 hours later when steady state diffusion was considered established. the composition of the electrolyte solution is described in table 2.as described in table 2 four various concentration sulfide ion added to the brine solution to investigate the poison effects on hydrogen permeation current and diffusivity. Hydrochloric acid or sodium chloride were added all solutions in order to adjust pH to approximately 7 before adding them to the permeation cell.

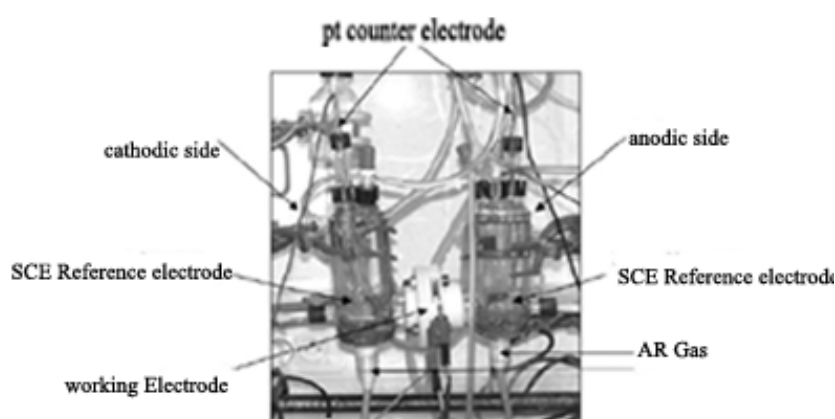


Fig.2. Experimental cell

Table 2.

composition of solution that used in hydrogen permeation test at 0.7 liter

Brine solution	Wt%	additives	C ₁	C ₂	C ₃	C ₄
NaCl	9.62	Na ₂ S,9H ₂ O gr	2.5	5.8	13.70	31.92
MgCl ₂	0.186					
CaCl ₂	0.305	CH ₃ COOH	1.2	2.61	6.08	14.1
Distilled water	89.89	(ml)				

2.2 data analysis

In this section the experimental results are presented. The results are discussed in view of a suggested surface poison effect by the sulfur compounds and an eventual retarding effect on the hydrogen absorption by sulfide film formation. for this study, the flux of hydrogen through the specimen was measured in terms of steady state current density I_{∞} (Am⁻²),and was converted to the steady-state hydrogen permeation flux, J_{∞} (mol m⁻² s⁻¹),according to the following equation and results directly from the Fick's first law:

$$J_{\infty} = (-D \frac{\partial c}{\partial x})_{x=L} = I_{\infty} / nf \quad 1$$

The permeation flux (mol m⁻¹s⁻¹) was defined by:

$$J_{\infty}L = I_{\infty}L / nf$$

2

where D is the hydrogen diffusion coefficient ($\text{m}^2 \text{s}^{-1}$) I_{∞} indicates the steady-state permeation current density, n the number of electrons transferred F the Faraday's constant, L (m) the specimen thickness and J_{∞} the steady state flux.

The following assumptions were made to derive a theoretical model for the hydrogen diffusion through the steel membrane. First it is assumed that the sample is effectively emptied of any residual hydrogen during the first 24 hours when the sample is polarized to 0 mV at the exit side with no solution in the charging cell. The initial hydrogen concentration in the steel membrane is therefore set to zero in the model. The boundary conditions are assumed to be constant and $C(0, t) = C_0$ at the entrance side and $C(L, t) = 0$ at the exit side for $t \geq 0$. The time when the cathodic potential is applied to the sample in the charging cell is defined as $t = 0$ in the model. The initial condition and the boundary conditions give the following expression for the hydrogen flux,

$$J(x, t) = DC_0 / L + 2DC_0 / L \sum [\cos(n \pi x / L) e^{-n^2 \pi^2 D t / L^2}] \quad 3$$

Where D is the diffusivity, $J(x, t)$ is the flux, C_0 is the subsurface hydrogen concentration, and L is the membrane thickness.[25].the effective hydrogen diffusivity, the rate limiting step D_{eff} ($\text{m}^2 \text{s}^{-1}$) is related to time lag by [25]

$$D_{\text{eff}} = L^2 / 6t_L \quad 4$$

Where t_L (s) is the lag time, defined as 0.63 times the steady state value, and D_{eff} determined by the transient t_L , if the surface hydrogen is in thermodynamic equilibrium with subsurface hydrogen[25], the hydrogen solubility C_{app} (mol m^{-3}) may be determined by

$$C_{\text{app}} = J_{\infty}L / D_{\text{eff}} \quad 5$$

3. Results and discussion

3.1 Typical permeation experiment/consecutive permeations

Fig. 3 shows the complete transient of hydrogen permeation experiment: after the required time for passivation of the exit side, the process begins when the extraction current density anodic (J_a) was stabilized for approximately 40 nA cm^{-2} (Fig. 4). On the entry side; with cathodic charging current applied (-2 mA cm^{-2}), a first rise transient was obtained; hydrogen transported through the sample was detected in the exit side (anodic cell) by potentiostat. It was usually illustrated that the typical curves permeation had a clear incubation time in the initial stage, then a region of constant gradient, and then finally became constant (state flux current of hydrogen I_p^{∞}). When the permeation rate achieved a steady-state level I_p^{∞} , the charging current was interrupted and the entry side of the membrane was polarized immediately at the same anodic potential as the exit side (0 mV) (Fig. 3).

Once, the flow of decay transient (discharging) established the base line, a second cathodic charging was carried out while being placed under the same galvanostatic conditions

described previously ($I_c = 2 \text{ mA cm}^{-2}$). (Fig. 3 second transient permeation). It was noted that the second transient permeation was slower than the first one. It presented a weaker current of permeation and a higher exit time: the slope of the curve of discharging at the beginning of the second charging was weaker than that of the curve of passivation at the beginning of the first charging (Figs. 3 and 5). The difference observed was attributed to mechanical polishing which causes a modification of the microstructure of surface by strain hardening. This hindered hydrogen transport and made effective hydrogen traps. The permeation was weaker during the second charging since the microstructure of the material has been changed due to hydrogen trapped during the first charging. However, on certain curves, we observed that the exit time of the second transient permeation was shorter than that of the first; which resulted in a more important slope of discharging. This phenomenon could be explained by admitting that the second charging started before the exit of the totality of hydrogen introduced into the sample during the first charging. If the hydrogen totality did not have time to allow outgassing, this phenomenon could be attributed to terms of irreversible trapping.

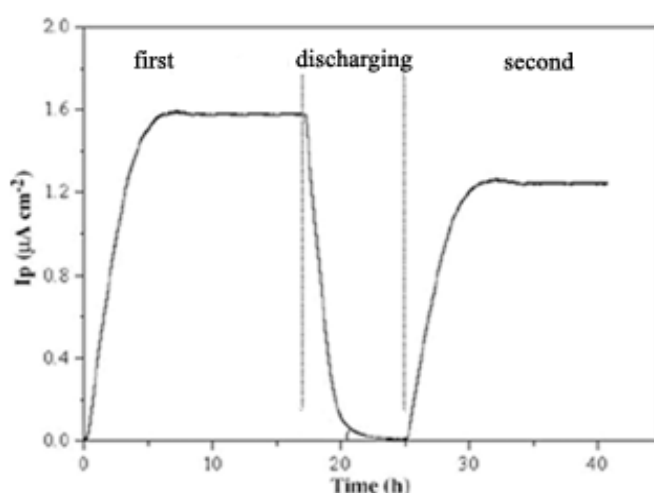


Fig.3. The hydrogen permeation charging and discharging curves of membrane iron.

It was usually illustrated that the typical curves permeation had a clear incubation time in the initial stage, then a region of constant gradient, and then finally became constant (state flux current of hydrogen I_p^∞). When the permeation rate achieved a steady-state level I_p^∞ , the charging current was interrupted and the entry side of the membrane was polarized immediately at the same anodic potential as the exit side (0 mV) Fig. 3.

Once, the flow of decay transient (discharging) established the base line, a second cathodic charging was carried out while being placed under the same galvanostatic conditions described previously ($I_c = 2 \text{ mA cm}^{-2}$). (Fig.3 second transient permeation). It was noted that the second transient permeation was slower than the first one. It presented a weaker current of permeation and a higher exit time: the slope of the curve of discharging at the beginning of the second charging was weaker than that of the curve of passivation at the beginning of the first charging (Figs.3 and 5). The difference observed was attributed to mechanical polishing which causes a modification of the microstructure of surface by strain hardening. This hindered hydrogen transport and made effective hydrogen traps. The permeation was weaker during the second charging since the microstructure of the material has been changed due to hydrogen trapped during the first charging. However, on certain curves, we observed that the exit time of the second transient permeation was shorter than that of the first; which resulted

in a more important slope of discharging. This phenomenon could be explained by admitting that the second charging started before the exit of the totality of hydrogen introduced into the sample during the first charging. If the hydrogen totality did not have time to allow outgassing, this phenomenon could be attributed to terms of irreversible trapping. The anodic current after the degassing of hydrogen was lower than the passivation current (current before the beginning of the first stage charging), which appeared logical since passivation continued during the permeation, from where the influence of the passivation time.

The significant different observed over time in exit between the first and the second transient permeation was probably due to the difference of the cathodic surface quality between the two charging. indeed, the passive layer present on cathodic surface before the first charging could behave in a way different from that of cathodic surface before the second charging. This probably indicated an evolution entry side face between two transient consecutive permeations: in particular, the modifications of the surface quality or the solution in the vicinity of surface.

3.2 Evidence of the influence of the passive layer on the exit side

To study the influence of the passive layer on the exit side, a series of experiments were carried out with the same sample. the best to obtain the good result to passivating the anodic side of the sample was observed by applying 0mv as a anodic polarization to the sample. This sample was repassivated in NaOH 0.1M solution between 70-78 ° for 1 h before the test. as illustrated in fig.4 anodic side get the less than 40 nA at the end of the polarization, and also if put the data in a log-log diagram the linear behavior of the curve will be observed. The passive layer formed on the surface of detection played a role of barrier to the permeation. It became more and more impervious, which explained the decrease of the characteristics (I_p^∞ , C_{app} , etc.) of the second permeation.

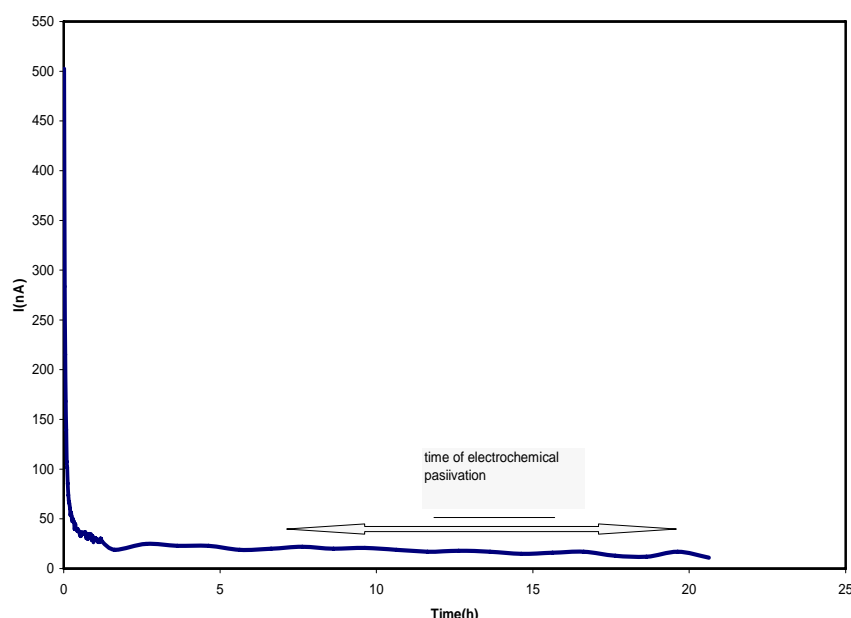


Fig.4. curve of electrochemical passivation of membrane iron potentiostatically maintained at a constant potential of 0 mv/SCE

What about was expected for hydrogen concentration (C_{app}) was to increase with increasing sulfide concentrations that was occurred in concentration C_1 to C_4 , but this trend can be seen on the contrary for concentration of C_3 which with increasing sulfide component concentration in solution reduction of hydrogen subsurface concentration was observed. That shows that hydrogen diffusion rate despite of increase in H_2S concentration in compare to solution C_1 are not increased. A reason for reduction of amount of hydrogen subsurface concentration is due to formation of iron sulfide layer (FeS) that is formed on the surface which Probably reduction of the amount of C_{app} in concentration C_3 is concern to stability of FeS layer in this concentration and potential which was observed the charged sides of the samples were black after 2 hours expose of sample that is due to the sulfide formation layer on the surface. However, any reason why ion sulfide should produce a more protective FeS film cannot be found. but sulfide ions in the concentration of C_4 , has increased hydrogen absorbed on the surface, so increasing the concentration cause to increase the amount of hydrogen that has been absorbed at all.

It is well known that adsorption of catalyst poisons, such as hydrogen sulphide, thiourea, arsenic compounds, etc., promotes the cathodic sorption of H into host metal lattices, such as Fe, Ti, Pd or Ni. many different mechanisms for the promotion of hydrogen sorption by surface poisons have been discussed by various authors and the following summary of the different ideas have been presented as[17, 26]: (a) additives such as Sb or As promote the hydrogen sorption by formation of (gaseous) hydrides; (b) the poisons increase the M–H bond strength; (c) 'colloidal particles', formed during electrolysis, promote entry of H; (d) in the presence of poisons, H can enter the host metal as injected protons; (e) poisons interfere with the H atom recombination step in cathodic H_2 evolution, thereby supposedly increasing the probability of H entry.

Usually, it is supposed that poisons block $H + H$ recombination to H_2 and thus favor entry of adsorbed H into the metal. However, this explanation seems ambiguous since poisons are also known to reduce pH owing to competition between poison and H for surface sites. The proposed mechanism of poisons as recombination blockers is therefore not entirely conclusive. A thermodynamic theory for the enhancement of H sorption by poisons including competitive adsorption have been proposed elsewhere [22,23], The theory explains how co adsorption of H and poisons increases the chemical potential of adsorbed H. The change in chemical potential for H when poisons are present compared to when they are absent is shown to be:

$$\mu_{\delta} = \mu_{0H(p)} - \mu_{0H} + RT \ln(1 + K_p C_p) \quad 6$$

where K_p is the chemical adsorption constant, and c_p is the concentration of the poison in the solution respectively. Since the driving force for sorption depends on the chemical potential of H at the surface it is shown that the enhanced hydrogen sorption can arise from fundamental thermo dynamical reasons. On the other hand, the data presented in this work indicate that the compound that is most prone to produce the HS^- anion also produces the highest increase in hydrogen absorption.

The analysis of the results enabled us to calculate the coefficient of diffusion by the time lag method with mathematical expression derived from Fick's second law [25]. In this investigation, the hydrogen diffusion coefficient, hydrogen trapping and apparent solubility of hydrogen measured in iron (0.1 M NaOH) defined by Eqs. (1)–(5) are presented in Table 3. For the samples, the mean value of the hydrogen diffusivity increased gradually from $9.37E-07$ to $10.95E-07 \text{ cm}^2 \text{ s}^{-1}$, as the test concentration C_1 to C_4 . The coefficients of diffusion values obtained were lower than those found for annealed iron ($8 \times 10^{-9} \text{ m}^2 \text{ s}^{-1}$) [26–28], but in

agreement with the values found with mechanically polished iron without annealing. Mechanical polishing induces a modification of the microstructure which leads to strain harden greatly the material surface provoking a decrease of hydrogen diffusivity.

Table3.

data of effective diffusivity D_{eff} , solubility hydrogen C_{app} versus different concentration during the permeation experiment.

Solution	$D_{\text{eff}} (\text{cm}^2 \text{ s}^{-1})$	$C_{\text{app}} (\text{mol/m}^3)$
C_1	9.3E-07	0.845
C_2	9.06 E-07	0.869
C_3	10.954E-07	0.719
C_4	7.5e-07	1.05

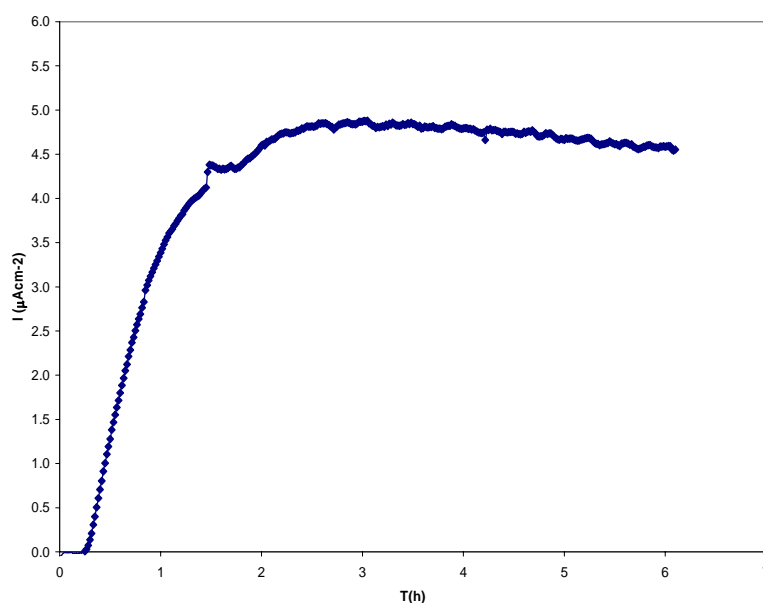


Fig.5. permeation charging curves of membrane iron

C_{app} or the ratio $J_{\infty}L/D_{\text{eff}}$ was calculated from Eq(5) and appeared to be highest for concentration C_4 and lowest for the concentration of C_3 . as mentioned before, with increasing the concentration C_1 to C_3 amount of hydrogen subsurface increased but in concentration C_3 we observed the critical behavior for hydrogen adsorption in this condition and after again increase at concentration C_4 . so this is obvious that hydrogen subsurface concentration adsorption in steel membrane increased due to the poisoning effect from HS^- on steel surface. In this way the highest value of the subsurface concentration is found representing the worst case. in some of the permeation curves, a maximum in the flux was recorded before a decrease to a lower steady state value occurred. In those cases the curve fit was performed on the data up to the maximum flux value. the maximum can have many different causes.

Hydrogen bubbles formed on the surface of the sample reduces the area exposed to the electrolyte, which decreases the hydrogen flux into the sample. Another explanation is that cavities are formed in the bulk of the sample. These cavities both traps hydrogen and also makes the diffusion path more tortuous [29].

This effect alters the apparent diffusivity for hydrogen in the sample. It should be noted that there is probably a quite large error in the presented concentration values but that they likely presents a reliable comparison between the effect of the different sulphur compounds.

4. Conclusion

The conclusions based on the data from this experimental campaign are presented below.

1. The simple diffusion model based on Fick's second law can be used to simulate hydrogen diffusion in steel A106 exposed to simulated sour solution that cathodically polarized.
2. The diffusion coefficient for H in A106 is approximately $9 \times 10^{-7} \text{cm}^2/\text{s}$ at 25°C .
3. The hydrogen uptake is generally higher when sulphur components are present at the charging side.
4. it is possible that iron sulphides formed at concentration about 1.7 mol and 2 mAcm^{-2} cathodic polarization reduces hydrogen absorption in the steel.
5. with review of literature 2mm thickness of the membrane iron that we used is distinguished in a thin thickness category, because the principal experimental results showed that hydrogen had easy mobility in this thickness and also for this thickness the concentration of solution C_3 is a critical in compare to others
6. it was also verified that the evaluation of the passive layer formed on the detection side during permeation acted as a barrier for hydrogen permeation, depending on time and electrochemical condition of the surface.

5. References

1. Q. Yang and J. Luo, Mat. Sci. Eng. A288 (2000) 75.
2. O. El kebir and A. Szummer, Int. J. Hydrogen Energy, 27 (2002) 793.
3. A. Głowacka and W. A. Swi_tnicki, Mat. Chem. Phys., 81 (2003) 496.
4. A. Głowacka and W. Swi_tnicki, J. Alloys Comp., 701 (2003) 356-357.
5. M. Hoelzel, S. Danilkin, H. Ehrenberg, D. Toeblens, T. Udovic, H. Fuess, and H. Wipf, Mat. Sci. Eng., A384 (2004) 255.
6. M. Wozniak, A. Glowacka, and J. Kozubowski, J. Alloys Comp. 404-406, 626 (2005).
7. D. Jones, Principles and prevention of corrosion, Macmillan Publishing company, 1992.
8. K. Førre, T. Hemmingsen, and S. Eliassen, Report (in Norwegian), Stavanger university college, 2003.
9. T. Hemmingsen, K. Førre, H. Urke, N. Aagotnes, and S. Eliassen, in proceedings, 13th scandinavian corrosion congress, Iceland, 2004.
10. S. Eliassen, Corr. Eng. Sci. tech., 39 (2004) 31.
11. H. Huang, W.J.D. Shaw, Corr. Sci. 34 (1993) 61.
12. H. Margot-Marette, G. Bardou, J.C. Charbonnier, Corr. Sci. 27 (1987) 1009.
13. G. Echaniz, C. Morales, T. Perez, Corr. 98 (1998) Paper No.120.
14. H.F. Lopez, R. Raghunath, J.L. Albarran, L. Martinez, Metall. Mater. Trans. A 27A (1996) 3601.
15. B. Beidokhti, A. Dolati, A.H. Koukabi, Materials science and engineering A 507 (2009) 167-173

17. K. Sieradzki, *Scripta metall.*, 15 (1981) 171.
18. M. Saenz de Santa Maria and A. Turnbull, *Corr. Sci.*, 29 (1989) 69.
19. A. Turnbull, M. Saenz de Santa Maria, and N. Thomas, *Corr. Sci.*, 29 (1989) 89.
20. D. Seeger and T. Boellinghaus, in *Corrosion 2003*, (NACE International, 2003) paper No. 03098.
21. U. Evans, *The Corrosion and Oxidation of Metals*, Edward Arnold (Publishers) Ltd., 1976, chap.11, p. 218.
22. T. Zakroczymski, *Hydrogen Degradation of Ferrous Alloys*, Noyes Publications, Park Ridge
23. (1985)
24. B. Conway and G. Jerkiewicz, *J. Electroanal. Chem.*, 357 (1993) 47.
25. G. Jerkiewicz, J. Borodzinski, W. Chrzanowski, and B. Conway, *J. Electrochem. Soc.*, 142 (1995) 3755.
26. G. Jerkiewicz, *Prog. Surf. Sci.*, 57 (1998) 137.
27. J. Crank, *The Mathematics of Diffusion*, Oxford University Press, (1957).
28. J.-L. Dillard, S. Talbot-Besnard, Determination of the diffusion of hydrogen by measuring the permeability in high purity iron, *Compt. Rend. Acad. Sci. (Paris).Ser. C* 269 (1969) 1173.
29. E.W. Johnson, M.L. Hill, *Trans. Met. Soc. AIME* 218 (1960) 1104.
30. B. Laveissiere, J.L. Philippart, J. Pagetti, *Electrochim. Acta* 36 (3=4) (1991) 615.
31. J. Bockris, M. Genshaw, and M. Fullenwider, *Electrochimica Acta*, 15 (1970) 47